

Design, Synthesis, and Biological Evaluation of Triazolo-pyrimidine Derivatives as Novel Inhibitors of Hepatitis B Virus Surface Antigen (HBsAg) Secretion

Wenquan Yu,^{†,‡,§} Cally Goddard,[‡] Elizabeth Clearfield,[‡] Courtney Mills,[‡] Tong Xiao,^{||} Haitao Guo,[§] John D. Morrey,[⊥] Neil E. Motter,[⊥] Kang Zhao,[†] Timothy M. Block,^{‡,§} Andrea Cuconati,^{*,‡,||} and Xiaodong Xu^{*,‡,||}

[†]School of Pharmaceutical Science and Technology, Tianjin University, Tianjin 300072, P. R. China

[‡]Institute for Hepatitis and Virus Research, Hepatitis B Foundation, Doylestown, Pennsylvania 18902, United States

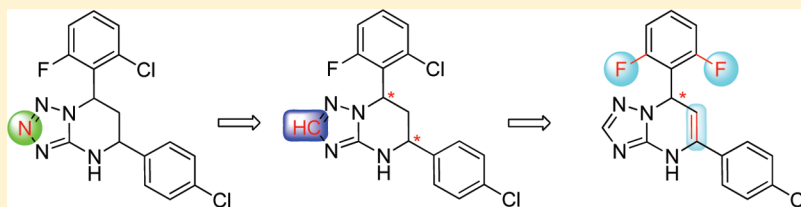
[§]Drexel Institute for Biotechnology and Virology Research, Drexel University College of Medicine, Doylestown, Pennsylvania 18902, United States

^{||}Pharmabridge, Inc., Doylestown, Pennsylvania 18902, United States

[⊥]Institute for Antiviral Research, Utah State University, Logan, Utah 84322, United States

 Supporting Information

ABSTRACT:



The high levels of hepatitis B virus (HBV) surface antigen (HBsAg)-bearing subviral particles in the serum of chronically infected individuals play an important role in suppressing HBV-specific immune response and are only mildly affected by the current small molecule therapies. Thus, a therapy that specifically reduces HBsAg serum levels could be used in combination therapy with nucleos(t)ide drugs or permit therapeutic vaccination for the treatment of HBV infection. Herein, we report the design, synthesis, and evaluation of novel triazolo-pyrimidine inhibitors (**1**, **3**, and **4**) of HBsAg cellular secretion, with activity against drug-resistant HBV variants. Extensive SAR led to substantial improvements in the EC_{50} of the parent compound, **5** (HBF-0259), with the best being **3c**, with $EC_{50} = 1.4 \pm 0.4 \mu M$, $SI \geq 36$. The lead candidates, both **1a** (PBHBV-001) and **3c** (PBHBV-2-15), were well-tolerated in both normal and HBV-transgenic mice and exhibited acceptable pharmacokinetics and bioavailability in Sprague–Dawley rats.

INTRODUCTION

Chronic hepatitis B affects more than 350 million people worldwide and is associated with as many as 1 million deaths per year due to the development of hepatocellular carcinoma, cirrhosis, and other complications.^{1–4} The current treatment options for hepatitis B include immune system modulation with two forms of interferon- α (IFN- α) and direct inhibition of the viral polymerase through five nucleos(t)ide analogues (Figure 1). Different versions of IFN- α show clinical benefit in up to 60% of patients but result in complete clearance in only 7%.^{5,6} However, there are several undesirable aspects to its use that render it far from ideal, chief among these being a high rate of adverse side effects that cause many patients to discontinue therapy.^{7,8} The FDA-approved small molecule drugs offer advantages over IFN- α including oral bioavailability, low toxicity, and efficacy in almost all patients, but complete clearance of infection (as measured by complete HBsAg and viremia loss) is rare and the emergence of resistance

remains a problem.⁹ Further development of effective therapeutics awaits antiviral drugs that target the viral life cycle through mechanisms other than inhibition of the viral polymerase, whether for monotherapy or combination therapy.¹⁰

One of the classic hallmarks of chronic hepatitis B is the high levels of hepatitis B virus surface antigen (HBsAg) in the serum of patients, which may reach 400 $\mu g/mL$ (0.4% of total serum protein).^{11,12} The antigenemia resulting from production of subviral particles is thought to play an important role in suppressing the HBV-specific immune response. In addition, recent reports have suggested that HBsAg acts directly on dendritic cells to limit cytokine production and adaptive immunity.^{13,14} Functionally, the role of HBsAg in eliciting HBV-specific immune tolerance has been demonstrated in woodchucks infected with

Received: December 3, 2010

Published: July 25, 2011

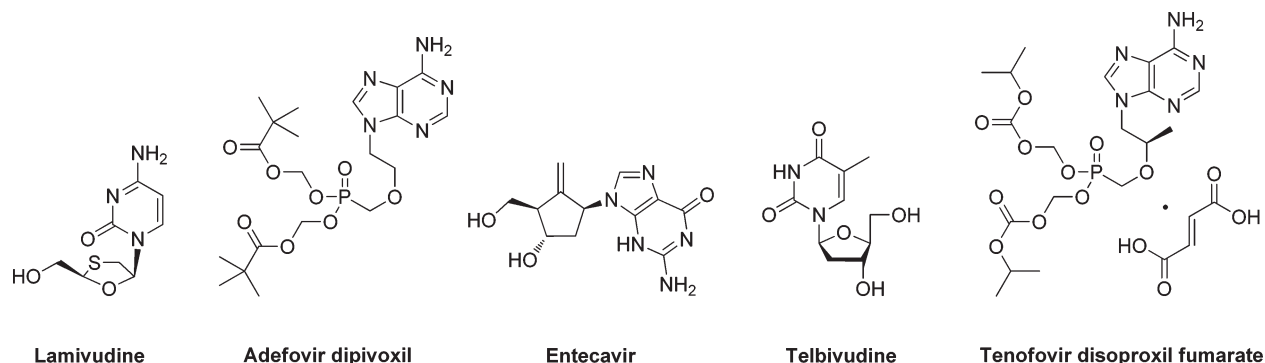


Figure 1. Nucleos(t)ide drugs approved by FDA for the treatment of chronic hepatitis B.

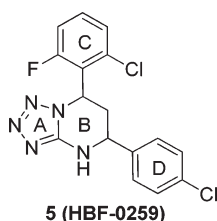


Figure 2. Structure of 7-(2-chloro-6-fluorophenyl)-5-(4-chlorophenyl)-4,5,6,7-tetrahydro-tetrazolo[1,5-*a*] pyrimidine **5**.

woodchuck hepatitis virus (WHV), an animal model that closely recapitulates chronic hepatitis B in humans. Reduction of antigenemia with the experimental antiviral clevudine resulted in a partial restoration of virus-specific immune response.¹⁵ Thus, inhibitors of HBsAg secretion^{16,17} could potentially enable the therapeutic use of the HBV vaccine or be used as combination therapy with nucleos(t)ide drugs for the treatment of HBV infection.

Our group is advancing the concept that control of HBsAg antigenemia, for which existing therapies have limited value, will be an important arm of future hepatitis B therapy regimens. Recently, we performed high-throughput screening of an in-house small-molecule library, using the HBV-expressing cell line HepG2.2.15, and identified 7-(2-chloro-6-fluorophenyl)-5-(4-chlorophenyl)-4,5,6,7-tetrahydro-tetrazolo[1,5-*a*]pyrimidine **5** (HBF-0259, Figure 2)¹⁸ as an effective inhibitor of HBV surface antigen secretion. Herein, we describe our followup lead optimization studies of a series of novel triazolo-pyrimidine inhibitors of HBsAg secretion, including the rational structure design, synthesis, and biological evaluation. The structure exploration involves the A, B, C, and D rings of **5** as shown in Scheme 1. In addition, biological profiles of selected compounds including activities against HBV mutants (**5**, **1a**, and **3c**), *in vivo* toxicity and pharmacokinetic (PK) studies (**1a** and **3c**) are also reported.

CHEMISTRY

Scheme 1 illustrates our strategy for the optimization of the original hit, **5**: (1) modification of the A ring to address the potential chemical stability issue of **5**, (2) structure exploration at the C and D side chains, and (3) understanding the effects of the chirality of the B ring on activity.

The tetrahydro-tetrazolo-pyrimidine structure of **5** could undergo rearrangement via the open azide form¹⁹ to give another

isomer, as shown in Scheme 2. To address this potential stability issue, the triazole analogue **1a**, by replacing N-2 with a CH group (on the A ring), was designed and synthesized to block the rearrangement process.

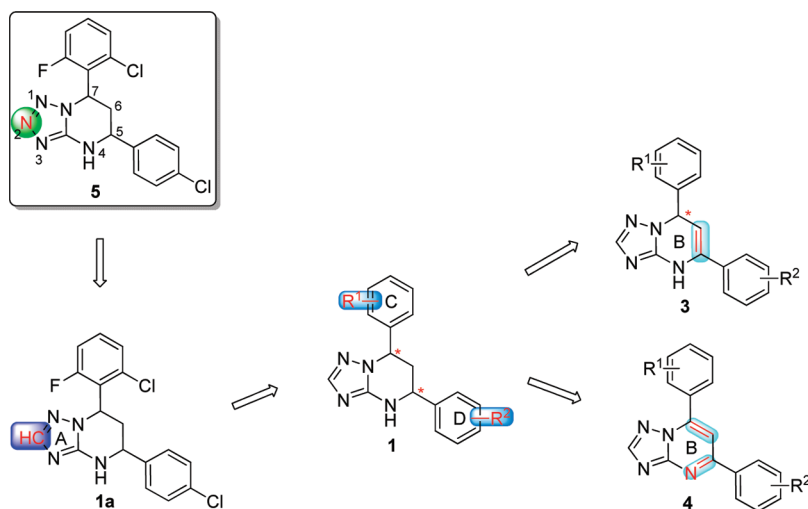
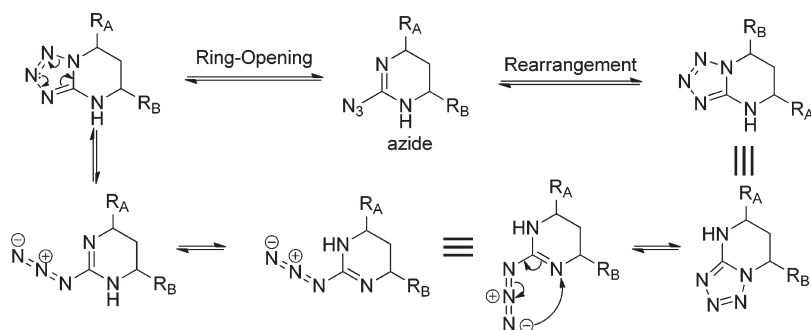
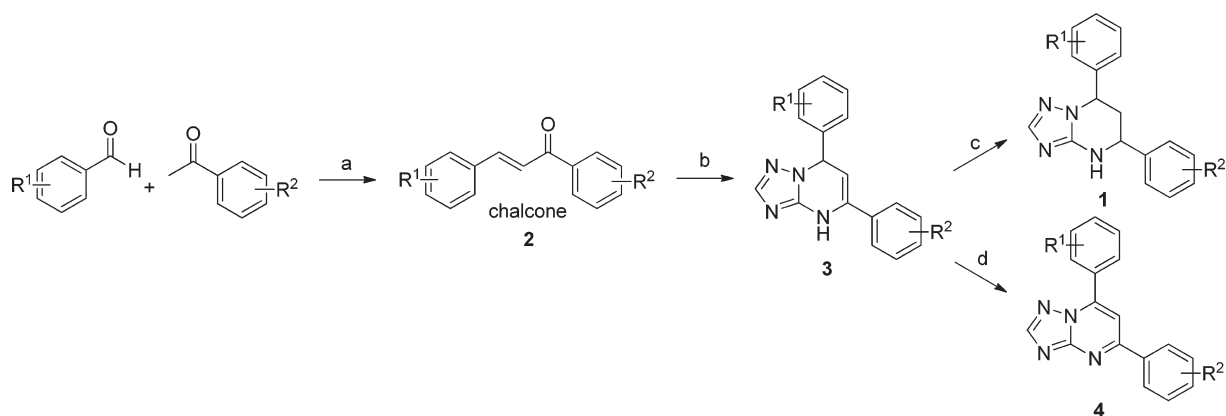
The synthetic sequence of **1a** and related triazolo-pyrimidine analogues **1**, **3**, and **4** was described in Scheme 3. Condensation of corresponding substituted benzaldehydes with acetophenones in the presence of sodium hydroxide in methanol, at room temperature, formed chalcones **2**.²⁰ Reaction of α,β -unsaturated ketones with 1*H*-1,2,4-triazol-3-amine in DMF at refluxing temperature gave dihydro-triazolo-pyrimidine analogues **3**, which were then reduced by sodium borohydride in methanol to afford tetrahydro-triazolo-pyrimidine analogues **1**.^{21,22} Analogues **4** were readily prepared through the oxidation of **3** with NBS.²¹ Although there are two chiral centers present in the molecule, the triazolo-pyrimidine analogues **1** exist only as a pair of thermodynamically more stable *cis*-enantiomers,^{23,24} evidenced by chiral HPLC (Figure 4) and NMR analysis. X-ray crystal structure of **1a** (Figure 3) confirmed that the C ring and D ring adopt the *cis*-conformation, while the tetrahydro-pyrimidine ring (B ring) adopts “half chair” conformation. Furthermore, the resolution of two enantiomers of **1a** was successfully carried out through chiral column chromatography (see Experimental Section).

RESULTS AND DISCUSSIONS

Inhibition of HBsAg Secretion. In the HepG2.2.15 cell line, the inhibitory activity (EC_{50}) and the cytotoxicity (CC_{50}) of **1a** were measured by the HBsAg ELISA and the MTT assay (Table 1), respectively, as we previously reported.¹⁸ The EC_{50} of **1a** for the inhibition of surface antigen secretion was $4.1 \pm 2.1 \mu\text{M}$, almost 3-fold more active than **5** ($EC_{50} = 11.3 \pm 3.2 \mu\text{M}$). No cytotoxicity was observed for either analogue up to the highest concentration tested ($50 \mu\text{M}$). Furthermore, inhibitory activity of HBsAg secretion was enantioselective and was only observed for the enantiomer **1** (Figure 4) of **1a** ($EC_{50} = 4.2 \pm 1.6 \mu\text{M}$), while the enantiomer **2** was largely inactive ($EC_{50} = 35.6 \pm 15.3 \mu\text{M}$).²⁵ Because neither of them exhibited cytotoxicity up to $50 \mu\text{M}$, all the other compounds were tested as a *cis* racemic mixture in the following study.

With this encouraging result in hand, we commenced exploration of the structure–activity relationship (SAR) on the side chains (C and D rings), based on triazolo-pyrimidine **1a**. Both EC_{50} s and CC_{50} s were investigated in the HepG2.2.15 cell line using the same assay described above. We did not observe cytotoxicity for any of these triazole analogues up to the highest

Scheme 1. Structure Exploration on A, B, C, and D Rings

Scheme 2. Ring-Opening and Rearrangement of the 4,5,6,7-Tetrahydro-tetrazolo[1,5-*a*]pyrimidineScheme 3. Synthesis of the Triazole Analogues 1, 3, and 4^a

^a (a) NaOH, MeOH, rt; (b) 1H-1,2,4-triazol-3-amine, DMF, reflux; (c) NaBH₄, MeOH, reflux; (d) NBS, ^tPrOH, reflux.

concentration tested (50 μ M) (Table 1). The SAR study on the C ring in compounds 1a–1r indicated that chloro/fluoro group at the *ortho* position (1a–e, compared with 1g) was necessary for the inhibitory activity of HBsAg secretion. The EC₅₀ was improved when the fluoro group was moved from the *ortho* (1a) to

the *para* (1d) position. Incorporation of an electron donating group (1f) instead of halides on the C ring decreased the potency. Compounds (1a and 1j–k) with halide groups at the *para* position on the D ring exhibited good EC₅₀s, with 4-bromo group (1k, EC₅₀ = 2.1 \pm 1.0 μ M) being the optimal one. The

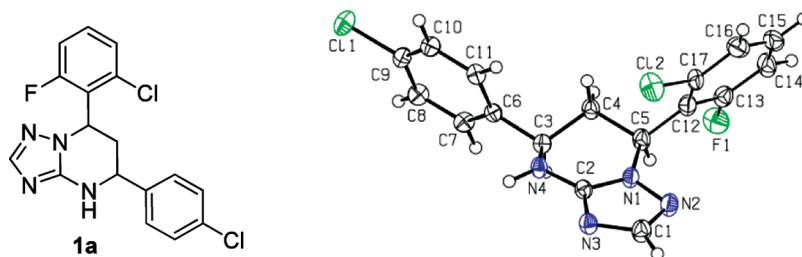


Figure 3. X-ray crystal structure of **1a**.

activity was maintained when the halide group was moved from the *para* (**1a**) to the *ortho* position (**1h**). However, the activity was decreased when the 4-halide group was moved to the *meta* position (**1i**) or replaced with electron donating groups (**1l–m**). Disubstitution (**1p–r**) on the D ring did not improve the inhibitory activities, except for the 2,3-dimethyl analogue (**1s**), which showed an EC_{50} of $2.2 \pm 0.5 \mu\text{M}$. Removal of the halide groups on the D ring (**1t**) significantly decreased the activity. Nevertheless, it is worth noting that biphenyl (**1n**) and 2-naphthyl (**1o**) analogues without halide substituents on the side chain exhibited significant potency. The introduction of a nitrogen atom to the D ring as shown in analogues **1u** and **1v** was associated with a loss of activity. This result could tentatively be attributed to the increased hydrophilicities (ClogP: **1u**, 2.37 and **1v**, 3.17 vs **1a**, 4.58), which may make it difficult for the compounds to pass through the cell membrane; alternatively, it is equally likely that interaction with a target binding site may also be affected.

Next, further structural modification on the core (B ring) of **1a** by introducing double bonds led to analogues **3a** and **4a**. Cell culture studies (Table 2) showed that **3a**, the precursor with only one chiral center for the synthesis of **1a** (Scheme 3), had a modest, but consistently better EC_{50} ($2.3 \pm 2.1 \mu\text{M}$) compared with **1a**. However, the nonchiral analogue **4a** completely lost its activity. To further investigate the scope of this observation, we tested more compounds with one chiral center (**3b–d** and **3h–s**). Compared with their corresponding analogues with two chiral centers, most of them (**3b–d**, **3i–j**, **3l–n**, and **3p–s**) exhibited better EC_{50} values. In this series, SAR study indicated 2,6-dihalide (**3a–3c**, compared with **3d**) was the optimal substituent on the C ring, and on the D ring, *para* (**3a**) and *meta* (**3i**) chlorination equally improved the activity. Overall, the best compound was the difluoro analogue (**3c**), which possessed an EC_{50} of $1.4 \pm 0.4 \mu\text{M}$, with minimum selectivity index (SI) of 36 ($CC_{50} > 50 \mu\text{M}$). This result indicated that the activities of the triazolo-pyrimidine analogues are very sensitive to the conformation of the molecule.

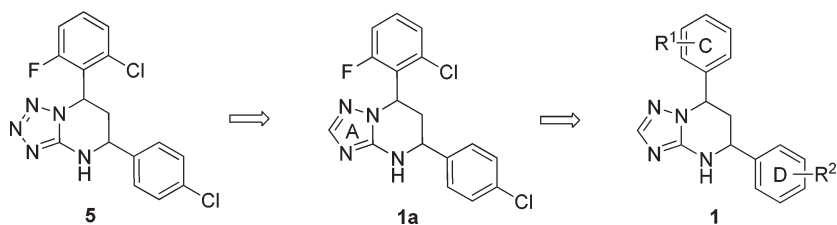
Assessment of Inhibitory Activity against Drug-Resistant HBV Strains. One of the problems associated with the current small molecule antiviral HBV medications is the emergence of drug resistant strains. The rate of resistant infection among the patient population varies with the drugs, ranging as high as 70% after three years of lamivudine/3TC treatment,²⁶ down to 5% after 2 years of entecavir treatment.^{27,28} However, lamivudine/3TC treatment predisposes patients to entecavir resistance, such that it occurs at 10% after 2 years²⁹ and 43% after 4 years.³⁰ This is due to the frequent acquisition of lamivudine/3TC resistance²⁶ and the subsequent partial cross-resistance to entecavir exhibited by the lamivudine resistant mutants. The newest approved drug, tenofovir, reportedly has had no verifiable resistance but has been

in widespread use for only two years, making firm conclusions on the emergence of resistance premature.

Resistance, which is due to mutations of the viral polymerase, leads to renewed clinical symptoms. It is thus extremely important that new HBV medications be evaluated for activity against drug resistant HBV strains, as this would be a desirable feature. Although the mechanism of action of **5** and its analogues appears distinct from the HBV polymerase inhibitors in clinical use, because of overlapping open reading frames, there are often HBsAg peptide changes that result from the emergence of polymerase drug resistant (DR) mutations,^{31,32} for instance, polymerase mutations M552 V, M552I, A529 V, T532G, and S550I result in the HBsAg alterations I195M, W196S, L173F, L176 V, and V194F, respectively. Thus, there is the possibility that the HBsAg of DR mutants may respond differently than the wild type to an inhibitor of HBsAg secretion. Therefore, the ability of the triazolo-pyrimidines to inhibit secretion of HBsAg from wild type and DR-HBV was compared.

To confirm activity against the DR mutants, **5**, **1a**, and **3c** were tested against representatives of the major classes of DR HBV strains, including lamivudine/telbivudine, adefovir, and entecavir resistant mutants. All but two of these mutants carry corresponding changes in HBsAg. For practical reasons, a transient transfection strategy was used rather than establishing stably transfected cell lines of each virus. The DR point mutations were introduced into a plasmid bearing a 1.3-mer HBV genome, subtype *ayw*, and the resulting constructs (plus wild type) were transfected into HepG2 cells. Following transfection, the cells were seeded into 96-well plates where they were treated with compounds in concentration from 50 to $0.016 \mu\text{M}$, in duplicate samples, and colorimetric HBsAg-specific capture ELISA was used to detect levels of secreted surface antigen. Interestingly, the secretion of HBsAg from wild type and DR strains in this transfection assay appears to be less sensitive than that in the HepG2.2.15 stable cell line, possibly due to increased levels of HBsAg expression in the transfected cells. However, **5**, **1a**, and **3c** all demonstrated significant activity against either wild type or DR mutants, confirming their possible utility in patients who have developed drug resistant strains (Table 3).

Assessment of Acute and Long-term Toxicity In Vivo. In preparation for in vivo pharmacokinetic and bioavailability studies, and eventual progression to efficacy studies in relevant animal models, we conducted a short-term acute toxicity study on **1a** and **3c**. Both analogues were selected as representatives of two structural classes that were superior to the parent compound **5**. CLS7BL/6 mice were administered a single intravenous bolus dose of each formulated compound at 25.0 and 7.9 mg/kg of **1a** and **3c**, respectively (maximum possible doses based on solubility limits), or vehicle alone. Over 24 h, neither compound caused observable morbidity, mortality, or weight loss. Blood cell counts

Table 1. SAR Study on A, C, and D Rings: EC₅₀s of 1a–v, Compared with 5^a

Compounds	C ring	D ring	ELISA, EC ₅₀ (μM)	MTT, CC ₅₀ (μM)
5	-	-	11.3 ± 3.2	> 50
1a			4.1 ± 2.1	> 50
1b			4.7 ± 1.9	> 50
1c			2.7 ± 1.0	> 50
1d			2.7 ± 0.7	> 50
1e			3.0 ± 0.7	> 50
1f			8.8 ± 3.2	> 50
1g			34.2 ± 13.6	> 50
1h			3.2 ± 1.8	> 50
1i			12.1 ± 3.6	> 50
1j			5.9 ± 3.3	> 50
1k			2.1 ± 1.0	> 50
1l			7.4 ± 1.7	> 50
1m			46.6 ± 3.2	> 50
1n			3.0 ± 1.3	> 50
1o			2.9 ± 0.7	> 50
1p			5.2 ± 1.9	> 50
1q			5.7 ± 1.9	> 50
1r			11.2 ± 2.2	> 50
1s			2.2 ± 0.5	> 50
1t			40.8 ± 15.9	> 50
1u			> 50	> 50
1v			> 50	> 50

^a EC₅₀: 50% effective concentration, measured by the HBsAg ELISA assay. CC₅₀: 50% cytotoxic concentration, measured by the MTT assay; both CC₅₀ and EC₅₀ are the average of at least two independent determinations.

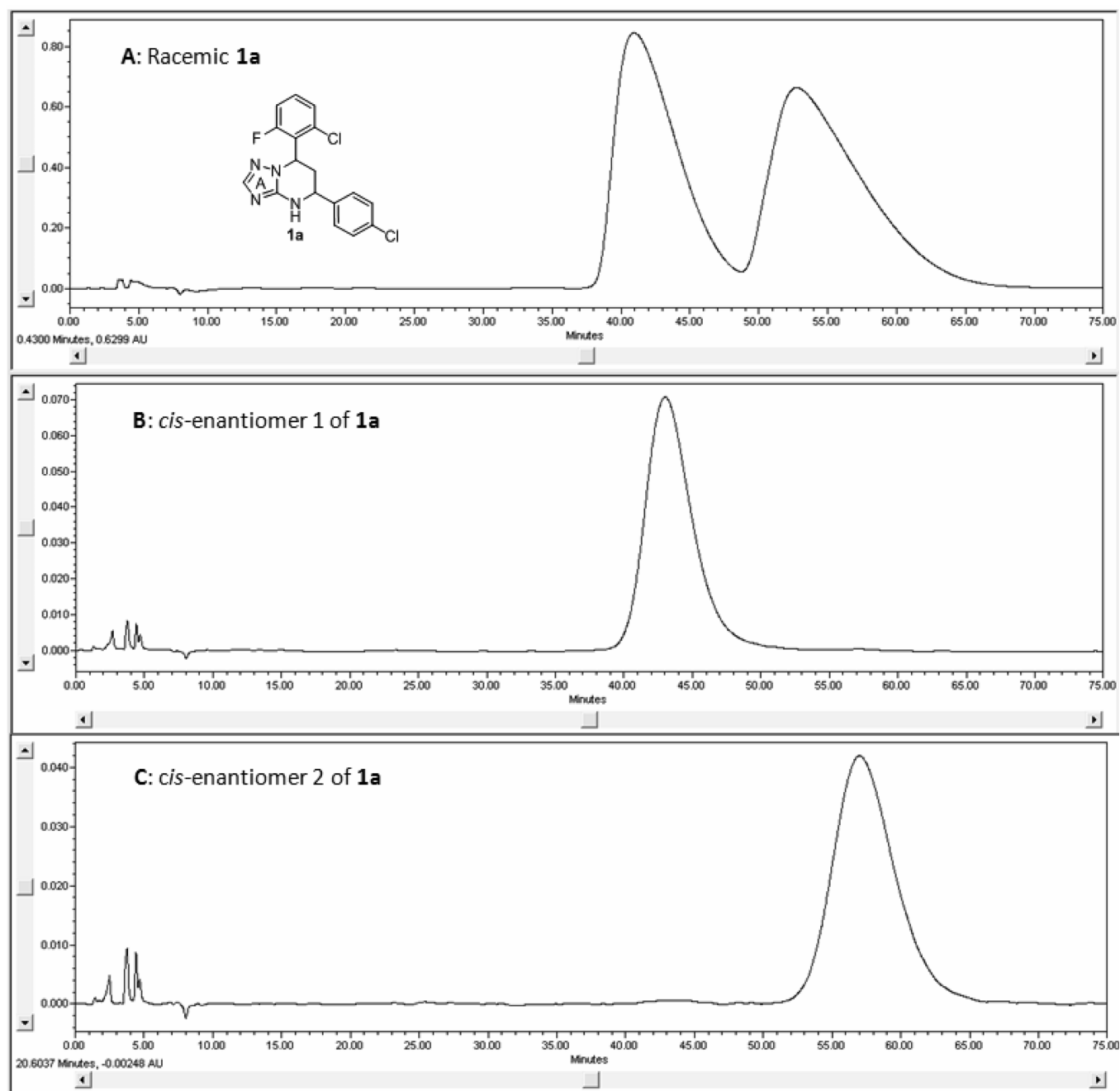


Figure 4. Chiral Resolution of Analogue 1a. (A) HPLC spectrum of racemic 1a; (B) HPLC spectrum of *cis*-enantiomer 1 of 1a; (C) HPLC spectrum of *cis*-enantiomer 2 of 1a.

were not affected in a statistically significant manner, although administration of 25 mg/kg of **1a** did show a trend toward reduction of platelets and neutrophils and also an increase in lymphocytes. Serum chemistry was unaffected by either compound (see Supporting Information).

To determine longer-term effects of exposure to **1a** and **3c**, HBV-transgenic mice (strain 1.3.32)³³ were used to approximate treatment in a disease-like physiological setting. It should be noted that due to overall low levels of serum HBsAg and highly variable expression, as well as a nonhuman cellular context, this model is not suitable for efficacy testing. Therefore, future studies will be conducted in a murine model in which chimeric human/

mouse livers support HBV infection and high levels of HBsAg secretion in a human cellular context.³⁴ Animals were dosed with the formulated compounds, or vehicle alone, by oral gavage once daily for 14 days. This study was carried after pharmacokinetic profiling and determination of oral bioavailability (described below). Oral dosing was used to simulate typical clinical use. No animals were observed to have died as a result of compound exposure, with some deaths in both vehicle and compound groups attributable to stress from the gavage procedure. No weight loss, morphological, or behavioral changes were noted in any treated animals. Treatment with **1a** resulted in elevated levels of alanine transaminase (ALT) and bilirubin in a minority of

Table 2. Further SAR Study on B ring: EC₅₀s of 3a–4a Compared with 1a and EC₅₀s of 3b–d and 3h–s^a

Compounds	C ring	D ring	ELISA, EC ₅₀ (μM)	MTT, CC ₅₀ (μM)
1a	-	-	4.1 ± 2.1	> 50
3a			2.3 ± 2.1	> 50
4a	-	-	> 50	> 50
3b			1.8 ± 1.2	> 50
3c			1.4 ± 0.4	> 50
3d			3.6 ± 2.0	> 50
3h			7.8 ± 3.2	> 50
3i			2.2 ± 0.9	> 50
3j			2.5 ± 1.2	> 50
3k			3.0 ± 1.6	> 50
3l			3.2 ± 1.2	> 50
3m			8.9 ± 3.6	> 50
3n			2.8 ± 2.1	> 50
3o			3.1 ± 1.4	> 50
3p			2.3 ± 1.3	> 50
3q			2.6 ± 0.9	> 50
3r			2.8 ± 2.0	> 50
3s			1.7 ± 1.1	> 50

^a EC₅₀: 50% effective concentration, measured by the HBsAg ELISA assay. CC₅₀: 50% cytotoxic concentration, measured by the MTT assay. Both CC₅₀ and EC₅₀ are the average of at least two independent determinations.

Table 3. Activity of Lead Compounds against HBsAg Secretion from HBV Mutants Bearing Drug Resistant Mutations^a

	resistance phenotype					
	genotype wild type EC ₅₀ (μM)	adefovir		lamivudine/telbivudine		entecavir
		genotype A529 V EC ₅₀ (μM)	genotype N584T EC ₅₀ (μM)	genotype M552I EC ₅₀ (μM)	genotype L528M/M552 V EC ₅₀ (μM)	genotype L528M/M552 V/T532G/S550I EC ₅₀ (μM)
5	32.0 ± 25.4	9.0 ± 2.6	5.6 ± 2.2	5.5 ± 1.6	14.2 ± 5.5	6.4 ± 2.5
1a	8.4 ± 2.3	5.8 ± 1.7	5.6 ± 1.8	9.1 ± 1.8	10.3 ± 8.2	8.3 ± 1.3
3c	6.9 ± 0.6	1.8 ± 0.5	6.4 ± 0.4	4.0 ± 0.5	8.5 ± 1.2	8.4 ± 3.7

^aEC₅₀: 50% effective concentration, the average of two independent determinations.

treated animals, indicating some loss of liver function. Both compounds caused a slight rise in total sodium. Treatment did not result in any other obvious and significant dose-dependent serum chemistry changes, with 3c being particularly inert (see Supporting Information).

Assessment of Pharmacokinetics In Vivo. After assessment of acute (24 h) toxicity in mice, the oral bioavailability and pharmacokinetics of 1a and 3c were evaluated in male Sprague–Dawley rats. Each test compound was administered intravenously at 5 mg/kg and orally at 25 mg/kg in fasted rats. Plasma concentrations of each test compound were determined by LC-MS/MS. Following intravenous dosing at 5 mg/kg, 1a had an average plasma half-life ($t_{1/2}$) of 2.17 ± 0.74 h. Its total body clearance rate (CL) was low, with an average value of 0.70 ± 0.19 L/h/kg, and its average volume of distribution (V_{ss}) was 1.6 ± 0.3 L/kg. After oral dosing at 25 mg/kg, 1a reached an average maximum plasma concentration (C_{max}) of 2437 ± 218 ng/mL, within an average time (T_{max}) of 2.3 h. The average bioavailability (F) was calculated at 31 ± 3% (see Supporting Information).

Following intravenous dosing at 5 mg/kg, 3c had an average plasma half-life ($t_{1/2}$) of 2.40 ± 0.38 h. Its total body clearance rate (CL) was moderate with an average value of 1.0 ± 0.4 L/h/kg, and its average volume of distribution (V_{ss}) was 2.6 ± 0.4 L/kg. After oral dosing at 25 mg/kg, 3c reached an average maximum plasma concentration (C_{max}) of 1937 ± 474 ng/mL, within an average time (T_{max}) of 4.0 h. The average bioavailability (F) was calculated at 42 ± 16% (see Supporting Information).

For both 1a and 3c, PK characteristics are favorable and suggest that an effective dosing regimen can be developed. In addition, oral bioavailability is likely underestimated due to the fact that a significant amount of the test compounds remained in the systemic circulation at the final collection time point (6 h) after oral dosing. Future studies will include later time points and/or a lower dosing concentration to allow for the determination of the elimination phase of the test compounds and a better estimation of the bioavailability.

CONCLUSION

The results of a cell-based phenotypic screen have led to a series of disubstituted triazolo-pyrimidines as novel and specific inhibitors of hepatitis B virus surface antigen (HBsAg) secretion. Although the exact mechanism of action is still under investigation and will be the focus of a future publication, the parent compound was shown to not be an inhibitor of viral genomic replication but rather a specific inhibitor of HBV envelope secretion. As such, the mechanism is distinct from the current hepatitis B small molecule drugs. In this work, we presented the results of

extensive SAR studies, which successfully improved the potency and chemical tractability of the parent compound. These triazolo-pyrimidine derivatives were also active in inhibiting HBsAg secretion of HBV variants that are resistant to current small molecule drugs. Selected lead analogues, both 1a (PBHBV-001) and 3c (PBHBV-2-15), were well tolerated in CL57BL/6 mice and displayed desirable pharmacokinetics profiles in male Sprague–Dawley rats. After 14 days of treatment of HBV transgenic mice, both 1a and 3c were fairly well tolerated, with 3c showing no signs of toxicity through serum chemistry analysis.

EXPERIMENTAL SECTION

Chemistry. ¹H NMR spectra were recorded on a 500 or 300 MHz INOVA VARIAN (75 MHz for ¹³C NMR; 282 MHz for ¹⁹F NMR) spectrometer. Chemical shifts values are given in ppm and referred as the internal standard to TMS (tetramethylsilane). The peak patterns are indicated as follows: s, singlet; d, doublet; t, triplet; q, quadruplet; m, multiplet; and dd, doublet of doublets. The coupling constants (J) are reported in hertz (Hz). Melting points were determined with a national micromelting point apparatus without corrections. Mass spectra were obtained on an Agilent LC-MS spectrometer (ES-API, Positive). Silica gel column chromatography was performed over silica gel 100–200 mesh, and the eluent was a mixture of ethyl acetate (EtOAc) and hexanes. All the tested compounds possess a purity of at least 95% as determined by HPLC. Analytical HPLC was run on the Agilent 1100 HPLC instrument, equipped with Phenomenex C12 column. Eluent system was: A (MeCN, 0.05%TFA) and C (H₂O, 0.05%TFA); flow rate = 1 mL/min. Method A: 60%A, 40%C, λ = 219 nm. Method B: 70%A, 30%C, λ = 254 nm. Method C: 80%A, 20%C, λ = 254 nm. Retention times (t_R) are given in minutes. Chiral resolution of compound 1a was carried out on the Waters 2695 HPLC instrument, equipped with CHIRALPAK AD-RH column. Eluent system was: 30%A (H₂O), 70%B (EtOH); flow rate = 0.5 mL/min; λ = 219 nm. (see Supporting Information for full experimental details and characterization data.)

a. Preparation of 1,3-Diaryl-propenone 2: General Procedure A. To a stirred solution of substituted benzaldehyde (20 mmol) and acetophenone (20 mmol) in methanol (15 mL) was added dropwise a solution of sodium hydroxide (26 mmol) in methanol (15 mL). The resulting mixture was stirred at room temperature for 6 h, then filtered and washed with water to yield the crude product. Pure compound 2 was got by recrystallization from methanol or through silica gel column chromatography (EtOAc/hexanes 2:98) as a light-yellow solid in 38–97% yield.

b. Preparation of 5,7-Diaryl-4,7-dihydro-[1,2,4]triazolo[1,5-a]pyrimidine 3: General Procedure B. A solution of 2 (5 mmol) and 3-amino-1,2,4-triazole (7.5 mmol) in DMF (5 mL) was refluxed for 2 h. The reaction mixture was cooled to room temperature, diluted with water (50 mL), and stirred sufficiently. The resulting mixture was filtered and washed

with water to give the crude product, which was further purified either by recrystallization from EtOAc or through silica gel column chromatography (EtOAc/hexanes 30:70) to afford **3** as a white solid in 41–92% yield.

5-(4-Chlorophenyl)-7-(2,6-difluorophenyl)-4,7-dihydro-[1,2,4]triazolo[1,5-*a*]pyrimidine (3c). The product was obtained according to general procedure B, as a white solid. Yield 83%; mp 223–224 °C. $R_f = 0.40$ (EtOAc/hexanes 50:50). MS: $MH^+ = 345$. 1H NMR (300 MHz, DMSO- d_6): δ 10.13 (s, 1H, NH), 7.66–7.61 (m, 3H, CH_{ar}), 7.49–7.41 (m, 3H, CH_{ar}), 7.13–7.07 (m, 2H, CH_{ar}), 6.63 (d, $J = 3.6$ Hz, 1H, $CH=C$), 5.26–5.25 (m, 1H, CH). ^{19}F NMR (282 MHz, DMSO- d_6): δ –118.26. ^{13}C NMR (75 MHz, DMSO- d_6): δ 160.6 (dd, $J_{C-F} = 247.9, 7.7$ Hz, C), 150.5 (C), 150.4 (C), 135.9 (C), 134.3 (C), 133.5 (CH), 131.4 (t, $J_{C-F} = 10.7$ Hz, C), 129.2 (CH), 128.4 (CH), 117.2 (t, $J_{C-F} = 15.2$ Hz, C), 112.8 (d, $J_{C-F} = 24.9$ Hz, CH), 95.1 (CH), 50.8 (CH). HPLC: 98.8% (method B, $t_R = 4.96$ min).

*c. Synthesis of 5,7-Diaryl-4,5,6,7-tetrahydro-[1,2,4]triazolo[1,5-*a*]pyrimidine 1: General Procedure C.* A sample of sodium borohydride (10 mmol) was added to a suspension of **3** (1 mmol) in methanol (5 mL). The reaction mixture was refluxed for 30 min, then cooled to room temperature, diluted with water (50 mL), and stirred sufficiently. The resulting mixture was filtered and washed with water to give the crude product, which was further purified by recrystallization from a mixture of EtOAc and hexanes to afford **1** as a white solid in 64–94% yield.

7-(2-Chloro-6-fluorophenyl)-5-(4-chlorophenyl)-4,5,6,7-tetrahydro-[1,2,4]triazolo[1,5-*a*]pyrimidine (1a). The product was obtained according to general procedure C, as a white solid. Yield 89%; mp 227–228 °C. $R_f = 0.16$ (EtOAc/hexanes 33.3:66.7). MS: $MH^+ = 363$. 1H NMR (500 MHz, DMSO- d_6): δ 7.54–7.15 (m, 8H, CH_{ar}), 5.98–5.94 (m, 1H, CH), 4.82–4.78 (m, 1H, CH), 2.47–2.13 (m, 2H, CH_2). HPLC: 99.8% (method A, $t_R = 3.67$ min).

*d. Synthesis of 7-(2-Chloro-6-fluorophenyl)-5-(4-chlorophenyl)-[1,2,4]triazolo[1,5-*a*]pyrimidine 4a.* A sample of NBS (299 mg, 1.68 mmol) was added to a solution of **3a** (101 mg, 0.28 mmol) in isopropyl alcohol (5 mL). The reaction mixture was refluxed for 36 h, then cooled to room temperature, treated with saturated $NaHCO_3$ solution (20 mL), and extracted with EtOAc (15 mL \times 3). The combined organic layer was dried over Na_2SO_4 and evaporated under reduced pressure. The given residue was purified through silica gel column chromatography (EtOAc/hexanes 30:70) to afford a 42 mg white solid of **4a** in 42% yield; mp 238–239 °C. $R_f = 0.33$ (EtOAc/hexanes 30:70). MS: $MH^+ = 359$. 1H NMR (500 MHz, $CDCl_3$): δ 8.48 (s, 1H, CH_{ar}), 8.15 (d, $J = 7.5$ Hz, 2H, CH_{ar}), 7.57–7.39 (m, 5H, CH_{ar}), 7.20–7.19 (m, 1H, CH_{ar}). HPLC: 97.9% (method C, $t_R = 5.47$ min).

Generation and Testing of Drug-Resistant HBV Variants. The plasmid pTREHBV, encoding the HBV genome of *ayw* serotype,³⁵ was used as the background wild type construct. Standard molecular biology procedures employing the GeneTailor site-directed mutagenesis system (Invitrogen, Carlsbad CA) were used to generate single or double point mutations that give rise to the following amino acid changes in the polymerase open reading frame: A529V, N584T, M552I, M552V, L528M/M552V, and L528M/M552V/T532G/S550L.^{31,32} To generate the double and quadruple mutants, nucleotide substitutions were introduced sequentially by generating single mutations, confirming the sequence, and introducing additional mutations into the intermediate construct. All constructs were confirmed by sequencing through Integrated DNA technologies (Coralville IA). Primer sequences used for mutagenesis are available upon request.

Transient expression of HBsAg from the mutant and wildtype HBV constructs was accomplished through transient transfection of plasmids into HepG2 cells seeded on 75 cm^2 flasks, using Lipofectamine 2000 reagent (Invitrogen) according to directions. Twenty-four hours following transfection, cells were harvested by trypsinization and reseeded into

96-well plates at a density of 5×10^5 cells/well. Twenty-four hours later, media in each well was replaced with media containing test compounds in concentrations ranging (in half-log steps) from 0.016 to 50.0×10^{-6} M, in 0.5% DMSO. Control wells contained DMSO alone. Each compound concentration was tested in duplicate. HBsAg levels was determined by ELISA assay,¹⁸ and EC_{50} values were calculated as described therein. For each mutant HBV genome, compounds were tested at least 5 and up to 10 times, allowing calculation of standard deviation.

Formulation for Intravenous Administration. To produce 2 mg/mL solutions for dosing, 2 mg of compound powders were initially dissolved in a 0.2 mL of 1:1 solution (volume: weight) of 1-methyl-2-pyrrolidinone (NMP, Sigma Aldrich): Solutol HS15 (BASF) with vortexing. After dissolution, 0.8 mL of sterile saline (0.95% NaCl in H_2O) was added slowly while vortexing. Solution was injected into test animals within 10 min of preparation.

Assessment of Toxicity In Vivo. The work was done at Utah State University. For the acute toxicity study, female C57BL/6 mice were randomized to the treatment groups, with four animals per group. **1a** and **3c** were prepared as detailed above for intravenous formulation and administered by tail vein injection at 25 and 7.9 mg/kg, with one group injected only with vehicle. Animals were observed closely for the initial hour following administration. After 24 h, animals were sacrificed and necropsied to examine for gross changes of internal organs, and whole blood and serum were collected for analysis of complete blood cell counts (CBCs, specifically red blood cells, white blood cells, platelets, lymphocytes, neutrophils, monocytes, percent eosinophils, percent basophils, hemoglobin, hematocrit, mean corpuscular volume, mean platelet volume, red cell distribution width, and mean corpuscular hemoglobin concentration, using a Hemavet 950FS, Drew Scientific, Anaheim, CA) and serum chemistry (alanine aminotransferase, blood urea nitrogen, creatinine, total bilirubin, albumin, alkaline phosphatase amylase, globulin, total protein, glucose, Ca^{2+} , Na^+ , K^+ , and phosphorus through a VetScan Chemistry, Electrolyte and T4 Analyzer, Abaxis, Union City, CA).

For the 14-day toxicity study, HBV-transgenic mice (strain I.3.32)³³ were randomized across groups with 10 mice per group. **1a** and **3c** were prepared as detailed above for intravenous formulation and administered by oral gavage at 25 and 7.9 mg/kg once daily for 14 days, with one group injected only with vehicle. Animals were weighed prior to first administration and after 3 days. Blood was collected from tail vein three hours prior to first administration at 7 days (three hours after administration) and after necropsis (three hours after last administration) at 14 days. Animals were observed closely for one hour for signs of distress after each administration. Serum chemistry (alanine aminotransferase, blood urea nitrogen, creatinine, total bilirubin, albumin, alkaline phosphatase amylase, globulin, total protein, glucose, Ca^{2+} , Na^+ , K^+ , and phosphorus through a VetScan Chemistry, Electrolyte and T4 Analyzer, Abaxis, Union City, CA).

Assessment of Pharmacokinetics and Bioavailability. This analysis was conducted under contract with Absorption Systems (Exton PA). Male Sprague–Dawley rats were randomized as to treatment group, with three animals per treatment (12 total). Two days prior to dosing, animals were surgically fitted with jugular vein cannulae for withdrawal of blood samples; for intravenous administration, a second cannula was fitted. At 12 h prior to dosing, animals were fasted but supplied with water. **1a** and **3c** were prepared as detailed above. For intravenous administration, animals were dosed at 5 mg/kg; for oral administration, animals were dosed at 25 mg/kg by gavage. Animals were observed for signs of distress throughout the procedure approximately 0.3 mL of whole blood were harvested from the cannulae at predosing time point, 5 min, 15 min, 30 min, 1 h, 3 h, and 6 h. Plasma was prepared, and quantitatively analyzed for test compounds by LC/MS after 8-point standard curve was established. Half-life, C_{max} , T_{max} , mean residence time, and bioavailability were calculated by standard methods.

■ ASSOCIATED CONTENT

S Supporting Information. Characterization data and NMR spectra of compounds **1**, **3**, and **4**; X-ray data of **1a** (CIF); in vivo data of **1a** and **3c**. This material is available free of charge via the Internet at <http://pubs.acs.org>.

■ AUTHOR INFORMATION

Corresponding Author

*For X.X.: phone, 215-589-6350; fax, 215-589-6316; E-mail, michaelxu@pharmabridgegroup.com. For A.C.: phone, 215-489-4918; fax, 215-489-4920; E-mail, acuconati.research@hepb.org.

■ ACKNOWLEDGMENT

This project was supported by the Commonwealth of Pennsylvania, the Hepatitis B Foundation, NIH grant 1R43AI077123-01A1, and NIH contract N01-AI50036.

■ ABBREVIATIONS USED

HBV, hepatitis B virus; HBsAg, hepatitis B virus surface antigen; SAR, structure–activity relationship; EC₅₀, 50% effective concentration; CC₅₀, 50% cytotoxic concentration; SI, selectivity index; IFN, interferon; FDA, Food and Drug Administration; WHV, woodchuck hepatitis virus; ELISA, enzyme-linked immunosorbent assay; MTT, 3-(4,5-dimethylthiazol-2-yl)-2,5-diphenyltetrazolium bromide; PK, pharmacokinetics; DR, drug resistant

■ REFERENCES

- (1) Lee, W. M. Hepatitis B virus infection. *N. Engl. J. Med.* **1997**, *337*, 1733–1745.
- (2) Hoofnagle, J. H. Therapy of viral hepatitis. *Digestion* **1998**, *59*, 563–578.
- (3) Robinson, W. S.; Klote, L.; Aoki, N. Hepadnaviruses in cirrhotic liver and hepatocellular carcinoma. *J. Med. Virol.* **1990**, *31*, 18–32.
- (4) Beasley, R. P. Hepatitis B virus. The major etiology of hepatocellular carcinoma. *Cancer* **1988**, *61*, 1942–1956.
- (5) Hollinger, F. B. Controlling hepatitis B virus transmission in North America. The North American Regional Study Group. *Vaccine* **1990**, Suppl: S122–S128; discussion: S134–S138.
- (6) Marcellin, P.; Lau, G. K.; Bonino, F.; Farci, P.; Hadziyannis, S.; Jin, R.; Lu, Z. M.; Piratvisuth, T.; Germanidis, G.; Yurdaydin, C.; Diago, M.; Gurel, S.; Lai, M. Y.; Button, P.; Pluck, N. Peginterferon alfa-2a alone, lamivudine alone, and the two in combination in patients with HBeAg-negative chronic hepatitis B. *N. Engl. J. Med.* **2004**, *351*, 1206–1217.
- (7) Hoofnagle, J. H.; di Bisceglie, A. M. The treatment of chronic viral hepatitis. *N. Engl. J. Med.* **1997**, *336*, 347–356.
- (8) Mailliard, M. E.; Gollan, J. L. Emerging therapeutics for chronic hepatitis B. *Annu. Rev. Med.* **2006**, *57*, 155–166.
- (9) Liaw, Y. F.; Chu, C. M. Hepatitis B virus infection. *Lancet* **2009**, *373*, 582–592.
- (10) Deres, K.; Schröder, C. H.; Paessens, A.; Goldmann, S.; Hacker, H. J.; Weber, O.; Krämer, T.; Niewöhner, U.; Pleiss, U.; Stoltefuss, J.; Graef, E.; Koletzki, D.; Masantschek, R. N. A.; Reimann, A.; Jaeger, R.; Gross, R.; Beckermann, B.; Schlemmer, K.; Haebich, D.; Rübsamen-Waigmann, H. Inhibition of hepatitis B virus replication by drug-induced depletion of nucleocapsids. *Science* **2003**, *299*, 893–896.
- (11) Heermann, K. H.; Goldmann, U.; Schwartz, W.; Seyffarth, T.; Baumgarten, H.; Gerlich, W. H. Large surface proteins of hepatitis B virus containing the pre-s sequence. *J. Virol.* **1984**, *52*, 396–402.
- (12) Hollinger, F. B.; Liang, J. T. Hepatitis B virus. *Fields Virology*, 4th ed.; Lippincott Williams & Wilkins: Philadelphia, 2001; pp 2971–3036.
- (13) Op den Brouwer, M. L.; Binda, R. S.; Geijtenbeek, T. B.; Janssen, H. L.; Woltman, A. M. The mannose receptor acts as hepatitis B virus surface antigen receptor mediating interaction with intrahepatic dendritic cells. *Virology* **2009**, *393*, 84–90.
- (14) Xu, Y.; Hu, Y.; Shi, B.; Zhang, X.; Wang, J.; Zhang, Z.; Shen, F.; Zhang, Q.; Sun, S.; Yuan, Z. HBsAg inhibits TLR9-mediated activation and IFN- α production in plasmacytoid dendritic cells. *Mol. Immunol.* **2009**, *46*, 2640–2646.
- (15) Menne, S.; Roneker, C. A.; Korba, B. E.; Gerin, J. L.; Tennant, B. C.; Cote, P. J. Immunization with surface antigen vaccine alone and after treatment with 1-(2-fluoro-5-methyl-beta-L-arabinofuranosyl)-uracil (L-FMAU) breaks humoral and cell-mediated immune tolerance in chronic woodchuck hepatitis virus infection. *J. Virol.* **2002**, *76*, S305–S314.
- (16) Korba, B. E.; Montero, A. B.; Farrar, K.; Gaye, K.; Mukerjee, S.; Ayers, M. S.; Rossignol, J. F. Nitazoxanide, tizoxanide and other thiazolidines are potent inhibitors of hepatitis B virus and hepatitis C virus replication. *Antiviral Res.* **2008**, *77*, 56–63.
- (17) Mahtab, M. A.; Bazinet, M.; Vaillant, A. REP 9AC: A potent HBsAg release inhibitor that can rapidly restore immunocompetence in patients with chronic hepatitis B. *The Liver Meeting (AASLD)* **2010**, 482.
- (18) Dougherty, A. M.; Guo, H.; Westby, G.; Liu, Y.; Simsek, E.; Guo, J.; Mehta, A.; Norton, P. G., B.; Block, T.; Cuconati, A. A substituted tetrahydro-tetrazolo-pyrimidine is a specific and novel inhibitor of hepatitis B virus surface antigen secretion. *Antimicrob. Agents Chemother.* **2007**, *51*, 4427–4437.
- (19) Desenko, S. M.; Gladkov, E. S.; Komykhov, S. A.; Shishkin, O. V.; Orlov, V. D. Partially hydrogenated aromatic substituted tetrazolo-[1,5- α]pyrimidines. *Chem. Heterocycl. Compd.* **2001**, *37*, 747–754.
- (20) Zhao, P.; Liu, C.; Huang, W.; Wang, Y.; Yang, G. Synthesis and fungicidal evaluation of novel chalcone-based strobilurins analogues. *J. Agric. Food Chem.* **2007**, *55*, 5697–5700.
- (21) Orlov, V. D.; Desenko, S. M.; Potekhin, K. A.; Struchkov, Y. T. Cyclocondensation of α,β -unsaturated ketones with 3-amino-1,2,4-triazole. *Chem. Heterocycl. Compd.* **1988**, *24*, 192–196.
- (22) Desenko, S. M.; Orlov, V. D.; Lipson, V. V.; Shishkin, O. V.; Lindeman, S. V.; Struchkov, Y. T. Imine–enamine tautomerism of dihydroazolopyrimidines. 3. 5-Aryl-substituted 4,7(6,7)-dihydro-1,2,4-triazolo[1,5- a]pyrimidines. *Chem. Heterocycl. Compd.* **1991**, *27*, 1242–1246.
- (23) Desenko, S. M.; Orlov, V. D.; Lipson, V. V. Chemical conversions of 5,7-disubstituted dihydro-1,2,4-triazolo[1,5- a]pyrimidines. *Chem. Heterocycl. Compd.* **1990**, *26*, 1362–1366.
- (24) Desenko, S. M.; Shishkin, O. V.; Orlov, V. D.; Lipson, V. V.; Lindeman, S. V.; Struchkov, Y. T. Synthesis and structure of 4,5,6,7-tetrahydro-1,2,4-triazolo[1,5- a]pyrimidines. *Chem. Heterocycl. Compd.* **1994**, *30*, 851–855.
- (25) The absolute stereochemistry of enantiomer **1** and **2** of compound **1a** has not been established.
- (26) Tipples, G. A.; Ma, M. M.; Fischer, K. P.; Bain, V. G.; Kneteman, N. M.; Tyrrell, D. L. Mutation in HBV RNA-dependent DNA polymerase confers resistance to lamivudine in vivo. *Hepatology* **1996**, *24*, 714–717.
- (27) Colonna, R. J.; Rose, R.; Baldick, C. J.; Levine, S.; Pokornowski, K.; Yu, C. F.; Walsh, A.; Fang, J.; Hsu, M.; Mazzucco, C.; Eggers, B.; Zhang, S.; Plym, M.; Kleszczewski, K.; Tenney, D. J. Entecavir resistance is rare in nucleoside naïve patients with hepatitis B. *Hepatology* **2006**, *44*, 1656–1665.
- (28) Tenney, D. J.; Levine, S. M.; Rose, R. E.; Walsh, A. W.; Weinheimer, S. P.; Discotto, L.; Plym, M.; Pokornowski, K.; Yu, C. F.; Angus, P.; Ayres, A.; Bartholomeusz, A.; Sievert, W.; Thompson, G.; Warner, N.; Locarnini, S.; Colonna, R. J. Clinical emergence of entecavir-resistant hepatitis B virus requires additional substitutions in virus already resistant to Lamivudine. *Antimicrob. Agents Chemother.* **2004**, *48*, 3498–3507.
- (29) Zoulim, F. Entecavir: a new treatment option for chronic hepatitis B. *J. Clin. Virol.* **2006**, *36*, 8–12.
- (30) Papatheodoridis, G. V.; Manolakopoulos, S.; Dusheiko, G.; Archimandritis, A. J. Therapeutic strategies in the management of patients with chronic hepatitis B virus infection. *Lancet Infect. Dis.* **2008**, *8*, 167–178.

(31) Seeger, C.; Mason, W. S. Hepatitis B virus biology. *Microbiol. Mol. Biol. Rev.* **2000**, *64*, 51–68.

(32) Yotsuyanagi, H.; Koike, K. Drug resistance in antiviral treatment for infections with hepatitis B and C viruses. *J. Gastroenterol.* **2007**, *42*, 329–335.

(33) Guidotti, L. G.; Matzke, B.; Schaller, H.; Chisari, F. V. High-level hepatitis B virus replication in transgenic mice. *J. Virol.* **1995**, *69*, 6158–6169.

(34) Utoh, R.; Tateno, C.; Yamasaki, C.; Hiraga, N.; Kataoka, M.; Shimada, T. C., K.; Yoshizato, K. Susceptibility of chimeric mice with livers repopulated by serially subcultured human hepatocytes to hepatitis B virus. *Hepatology.* **2008**, *47*, 435–446.

(35) Guo, H.; Jiang, D.; Zhou, T.; Cuconati, A.; Block, T. M.; Guo, J. T. Characterization of the intracellular deproteinized relaxed circular DNA of hepatitis B virus: an intermediate of covalently closed circular DNA formation. *J. Virol.* **2007**, *81*, 12472–12484.